Annals of Nuclear Medicine Vol. 18, No. 7, 563–572, 2004

Evaluation of the use of a standard input function for compartment analysis of [^{123}I]iomazenil data: factors influencing the quantitative results

Yujiro SEIKE,*1 Kazuo HASHIKAWA,*2 Naohiko OKU,*3 Hiroshi MORIWAKI,*4 Haruko YAMAMOTO,*4 Kazuki FUKUCHI,*5 Yoshiyuki WATANABE,*6 Masayasu MATSUMOTO,*7 Masatsugu HORI*8 and Tsunehiko NISHIMURA*9

*1*Strokology Medical Department, Bobath Memorial Hospital*
*2*Department of Brain Imaging, Human Brain Research Center, Graduate School of Medicine, Kyoto University*
*3*Department of Nuclear Medicine and Tracer Kinetics, Osaka University, Graduate School of Medicine*
*4*Cerebrovascular Division, National Cardiovascular Center*
*5*Department of Radiology and Nuclear Medicine, National Cardiovascular Center*
*6*Department of Medical Robotics and Image Sciences, Osaka University Graduate School of Medicine*
*7*Department of Clinical Neuroscience and Therapeutics, Hiroshima University*
*8*Department of Internal Medicine and Therapeutics, Osaka University Graduate School of Medicine*
*9*Department of Radiology, Graduate School of Medical Sciences, Kyoto Prefectural University of Medicine*

Adoption of standard input function (SIF) has been proposed for kinetic analysis of receptor binding potential (BP), instead of invasive frequent arterial samplings. The purpose of this study was to assess the SIF method in quantitative analysis of [^{123}I]iomazenil (IMZ), a central benzodiazepine antagonist, for SPECT.

SPECT studies were performed on 10 patients with cerebrovascular disease or Alzheimer disease. Intermittent dynamic SPECT scans were performed from 0 to 201 min after IMZ-injection. BPs calculated from SIFs obtained from normal volunteers (BP_s) were compared with those of individual arterial samplings (BP_o).

Good correlations were shown between BP_os and BP_ss in the 9 subjects, but maximum BP_ss were four times larger than the corresponding BP_os in one case. There were no abnormal laboratory data in this patient, but the relative arterial input count in the late period was higher than the SIF. Simulation studies with modified input functions revealed that height in the late period can produce significant errors in estimated BPs.

These results suggested that the simplified method with one-point arterial sampling and SIF can not be applied clinically. One additional arterial sampling in the late period may be useful.

Key words: [^{123}I]iomazenil, SPECT, kinetic analysis

INTRODUCTION

The [^{123}I]iomazenil (IMZ) used in single photon emission tomography (SPECT) scans has high affinity for central benzodiazepine receptors.[1–6] Since central benzodiazepine receptors play an important role in brain function, evaluating their concentration has proved useful in localizing epileptogenic foci[7,8] as well as lesions in psychiatric disorders,[9–12] cerebrovascular disease,[13] and neurodegenerative disease.[14–16] In particular, in the analysis of degenerative disease, quantitative benzodiazepine receptor values might play an important role because benzodiazepine receptors may be decreased throughout the brain in degenerative diseases.

Many methods for the quantitative assessment of neuroreceptors by positron emission tomography (PET) or SPECT have been reported, and they have generally been either equilibrium-based analyses or kinetic analyses.

Tracer kinetic analysis[17,18] has usually been used to

Received June 6, 2003, revision accepted May 27, 2004.

For reprint contact: Yujiro Seike, M.D., Strokology Medical Department, Bobath Memorial Hospital, 1–6–5 Higashinakahama, Joto-ku, Osaka 536–0023, JAPAN.

E-mail: Seike@omichikai.or.jp

extract quantitative information from the data acquired. This method allows the binding potential (BP)[17] to be determined by a single bolus injection,[19–23] but it requires frequent arterial blood samplings and separation of the lipophilic component from each sample. The former is painful for patients, and the latter laborious for investigators. Accordingly, use of the SIF determined from healthy subjects' data has been reported to be one means of avoiding these inconveniences. Nevertheless, it has not been demonstrated that the average arterial time activity curve (TAC) of healthy normal volunteers yields correct results when applied to analysis of patients.

In the present study, we investigated the feasibility of using standard input function (SIF) instead of an individual patient's input function in compartment analysis of IMZ.

THEORY

A 3-compartment model[20,24] was employed to analyze tissue tracer kinetics in this paper, the three compartments being the arterial plasma compartment, the free and nonspecific binding compartment, and the specific binding compartment. The nonspecific binding compartment of IMZ in brain tissue was assumed to rapidly equilibrate with the free component.

The ligand concentration in each compartment is given by

$$\frac{dC_{F+NS}(t)}{dt} = K_1C_P(t) - (k_2 + k_3)C_{F+NS}(t) + k_4C_S(t) \quad \text{Eq. 1}$$

$$\frac{dC_S(t)}{dt} = k_3C_{F+NS}(t) - k_4C_S(t) \quad \text{Eq. 2}$$

where C_P is the concentration of extractable ligand in arterial plasma, C_{F+NS} is that of the free and nonspecific binding compartment, C_S is that of ligand bound specifically, K_1 is the rate constant of the blood-to-brain transport of ligand, k_2 is that of the brain-to-blood transport of ligand, k_3 is that of the association, and k_4 is that of the dissociation.

Total concentration in the tissue (C_T) is expressed by

$$C_T(t) = C_{F+NS}(t) + C_S(t) \quad \text{Eq. 3}$$

$$= \frac{K_1}{\alpha_2 - \alpha_1}\left\{(k_3+k_4-\alpha_1)e^{-\alpha_1 t}+(\alpha_2-k_3-k_4)e^{-\alpha_2 t}\right\}\otimes C_P(t) \quad \text{Eq. 4}$$

$$\alpha_1 = \frac{k_2 + k_3 + k_4 - \sqrt{(k_2 + k_3 + k_4)^2 - 4k_2k_4}}{2} \quad \text{Eq. 5}$$

$$\alpha_2 = \frac{k_2 + k_3 + k_4 + \sqrt{(k_2 + k_3 + k_4)^2 - 4k_2k_4}}{2} \quad \text{Eq. 6}$$

where $\otimes$ represents the mathematical operation of convolution. We used the SIF derived from six normal volunteers' arterial curves.[25]

BP[17] can then be defined as

$$BP = \frac{B_{max}}{K_D} = \frac{K_1k_3}{f_1k_2k_4} \quad \text{Eq. 7}$$

where B_{max} is receptor density, K_D is affinity, and f_1 is the free fraction of the parent compound in the plasma.

MATERIAL AND METHODS

Subjects. SPECT studies were performed on 34 patients with cerebrovascular disease (19 males and 3 females; age range 39–78 years), Alzheimer's disease (5 males and 5 females; age range 55–78 years), or epilepsy (2 males; age 18 and 19 years). The diagnoses were verified by CT or MRI and the clinical course. The clinical manifestations in the Alzheimer's cases fulfilled the criteria for probable Alzheimer's disease proposed by NINCDS-ADRDA.[26] None of the subjects were being treated with benzodiazepine derivatives. Informed consent was obtained from each subject, and the study was approved by the local ethics committee. No side effects were observed in any of the subjects after administration of IMZ. Plasma time activity curve (pTAC) were obtained in 26 patients and detailed pTAC were obtained in 10 male patients (9 patients with previous cerebral infarction, 1 patient with Alzheimer's disease; age range 52–78 years), and compartment analyses were applied to these 10 patients' data. Eight patients had only SPECT scans taken and their tissue TAC (tTAC) were compared with the others.

Radiopharmaceuticals. IMZ was supplied by Nihon Medi-Physics Co., Ltd. (Hyogo, Japan). Each vial contained 111 MBq of ^{123}I bound to 0.5 μg (1.2 nmole) of IMZ. Its specific activity was approximately 92.5 TBq/mmole at administration, and the radiochemical purity was greater than 95%.

Imaging protocol. The subject rested on the table in the supine position with eyes closed. The room was dimly lit, and ambient machine noises were kept to a minimum. The subject's head was immobilized with a ready-made plastic headholder so that the external auditory meatuses were aligned to the machine's built-in positioning crossed-light beam.

Prior to scanning, after subcutaneous local anesthesia with 1% lidocaine, a 22-gauge canula was inserted into the left radial artery, and each subject was given an intravenous bolus injection of 83–109 MBq of IMZ. In 10 patients arterial blood samples were drawn manually at 10-sec intervals during the first 1 min, and thereafter at 1.5, 2, 5, 7.5, 10, 15, 30, 45, 60, and 180 min post-injection. The plasma was separated from the whole blood samples by centrifugation, and the lipophilic fraction was extracted from the arterial plasma with octanol. The

residual counts after octanol extraction were measured with a gamma well counter. In this study, the radioactivity of the lipophilic component extracted by octanol from plasma was considered representative of the true arterial input function.[23,27]

Dynamic SPECT scans were performed three times. The first dynamic SPECT scan consisted of 16 frames and was performed from the time of injection until 42 min post-injection. The second 21-min dynamic scan consisted of 8 frames and was started at 90 min, and the final 21-min dynamic scan consisted of 8 frames, started 180 min post-injection. Each SPECT acquisition was performed in 64 steps, 360 degrees. The SPECT scanner used was a high-performance, four-head gamma camera (Hitachi Medico, Co., Japan) equipped with low-energy, general-purpose, parallel-hole collimators. The spatial resolution of the reconstructed system was 13 mm full-width-half-measure. The number of projections was 64, and the acquired matrix was 64 × 64 (pixel size: 4 × 4 mm). The 8-mm slice transaxial images were reconstructed using a Butterworth filter as the reconstruction filter. Chang's postreconstruction attenuation correction was applied with an attenuation coefficient of 0.08 cm^{-1} to the transaxial image data. Image slices were reconstructed parallel to the orbito-meatal line. A cross-calibration scan was performed using a cylindrical uniform 16-cm phantom filled with ^{123}I to calibrate sensitivity between the SPECT scanner and the well counter system. The subjects' ears were marked so that their head position was kept constant for all three SPECT scans.

Regions of interest. Regions of interest (ROIs) were defined over the right and left frontal, temporal, parietal, and occipital cortices, and over the cerebellum, thalamus, and basal ganglia. Square ROIs whose edge length is 2 cm were used, and the corresponding tTAC curves were calculated.

Input function. SIF had been previously acquired in 6 normal healthy volunteers.[25] A calibrated arterial TAC ($C_a(t)$) was obtained according to Eq. 8 and Eq. 9.

$$C_a(t) = f_{c0} \cdot C_s(t) \qquad \text{Eq. 8}$$

$$C_a(30) = A(30) \qquad \text{Eq. 9}$$

where f_{c0} is the calibration factor to scale SIF in each study and $C_s(t)$ is the activity of SIF; A(30) is the value of the original arterial TAC at 30 min post-injection of IMZ. BP was estimated on the basis of the 3-compartment-3-parameter model.

Data analysis. In the present study, a 3-compartment-3-parameter model analysis was applied to quantify BP. In the calculations, the K_1/k_2 value was assumed to be a constant ratio of 3 m*l*/g, which is roughly compatible with the values previously reported in human studies.[23] The previously reported free fraction IMZ values in arterial blood (f_1; Eq. 7) were 0.23[21] and 0.24.[23] A fixed f_1 value of 0.24 was used in this study. The radioactivity of the intravascular space in brain tissue was neglected in this study, because it was estimated to be in the order of 3–4% of brain tissue.[28] The difference between the time when IMZ reached the radial artery and time when IMZ reached brain tissue was set to 0 min. Sequential quadratic programming[29,30] was applied to solve the nonlinear equations with constraints of practical positive values ($0 < K_1$, k_2, $k_4 < 1$ and $0 < k_3 < 2.5$) using MATLAB and optimization TOOLBOX software (The Mathwork Inc., USA).

The nonlinear equations were solved using initial value (K_1, k_2, k_3, k_4) = (0.15, 0.05, 0.05, 0.026). Results were rarely divergent (1.4%); however, proper initial value gave the same answer. Minor variations (from 0.5 to 2 times) of initial value gave the same K_1, k_2, k_3, k_4, and BP. Fitting error between actual tTAC and calculated tTAC was checked by visual analysis with a TAC graph at every calculation of nonlinear equations. There were no outliers in tTACs of all ROIs.

We defined SD2MAX as fitting error of tTAC.

$$\text{SD2MAX} = \frac{\sqrt{\sum_{i=1}^{n} (y_{ai} - y_{ci})^2}}{n \cdot \text{MAXtTAC}^2} \qquad \text{Eq. 10}$$

where y_a is an actual count of tTAC, y_c is a calculated count, MAXtTAC is the max count of tTAC, and n is the number of tTAC measurements. In this study, SD2MAX was 0.043 (SD; 0.015) in the ten patients. Dynamic SPECT scans were performed three times and this did not worsen the fitting errors.

Simulation

The simulation below was performed to check the robustness of SIF. We selected three factors: peak value (value of the pTAC in the early period), peak time, and decay rate in the late period. In this paper the early period was taken to be that from injection time to the calibration time, and the late period as that from the calibration time to the end of the SPECT scan.

Change in the peak value of pTAC in the early period. The value of the original pTAC was modified by multiplying it by 0.3, 0.8, 1.5, or 2.0 times 0–30 min post-injection (Fig. 1A). The value of the modified pTAC from 30 to 180 min was the same as the original.

$$C_a(t) = f_c(t, \alpha) \cdot C_s(t) \qquad \text{Eq. 11}$$

$$f_c(t, \alpha) = \frac{(\alpha - 1) \cdot t}{t_p} + 1 \qquad (0 \le t < t_p) \qquad \text{Eq. 12}$$

$$f_c(t, \alpha) = \frac{(\alpha - 1) \cdot (30 - t)}{30 - t_p} + 1 \qquad (t_p \le t < 30 \text{ min}) \qquad \text{Eq. 13}$$

$$f_c(t, \alpha) = 1 \qquad (30 \text{ min} \le t) \qquad \text{Eq. 14}$$

α = 0.3, 0.8, 1.5, or 2.0

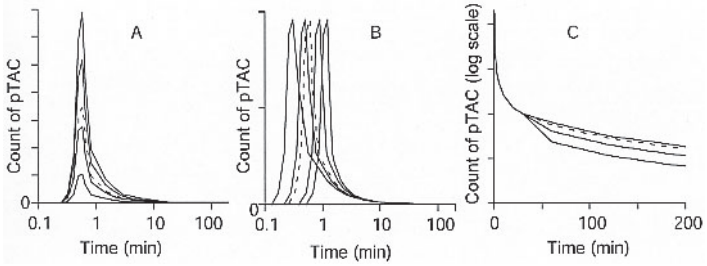

Fig. 1 Simulation model of input function. (A) The value of the original time activity curve in plasma (pTAC) was modified by multiplying it by 0.3, 0.8, 1.5, or 2.0 times 0–30 min post-injection according to Eq. 11–14. (B) The peak time of standard input function (SIF) was 0.54 min. In the modified pTAC, the peak count time in pTAC shifted to 0.3, 0.5, 0.9, and 1.2 min. (C) The original pTAC were multiplied by 0.4, 0.7, and 1.1, 30–180 min post-injection, and had the same value 0–30 min post-injection. The dashed line represents the original curve.

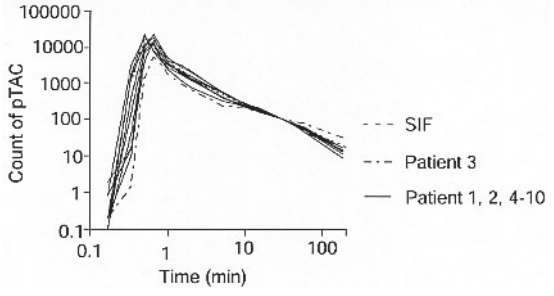

Fig. 2 The pTAC of SIF and 10 patients. Counts shown in this figure are calibrated with the count at 30 min post-injection set equal to 100.

where t_p is the count peak time in pTAC.

The multiplication factors (α) were made slightly larger than their actual variability determined in our cases and in earlier studies.[25]

Changes in peak time of pTAC. The peak time of SIF was 0.54 min. In the modified pTAC, the peak count time in pTAC shifted to 0.3, 0.5, 0.9, and 1.2 min (Fig. 1B). TAC 30–180 min post-injection was the same as the original pTAC. The peak count in each modified TAC was set to the same value of that of the original pTAC.

Changes in the late period of pTAC. To examine the influence of washout from the blood pool, we changed the value of the late period of pTAC. The original TAC were multiplied by 0.4, 0.7, and 1.1, 30–180 min post-injection, and they had the same value 0–30 min post-injection (Fig. 1C). We were unable to determine the results when the multiplication factor was greater than 1.1, because the counts of pTAC either did not change or became greater than that at 30 min. Such situations never occur when actual measurements are made.

$$C_a(t) = f_c \cdot C_s(t) \qquad \text{Eq. 15}$$

$$f_c = f_{c0} \cdot f_m \qquad \text{Eq. 16}$$

$$f_m = 1 \qquad (0 < t \le 30 \text{ min}) \qquad \text{Eq. 17}$$

$$f_m = 0.4, 0.7, 1.1 \qquad (30 < t \le 180 \text{ min}) \qquad \text{Eq. 18}$$

In the region where BP_s was very different from BP_o in patient 3, the peak count time of tTAC occurred more than 40 min later, and for that reason we checked the influence of peak count time in tTAC on estimation of BP.

Changes in peak count time of tTAC. To determine whether peak count time of tTAC influenced BP, we set the peak count times of tTAC in the range from 5 to 140 min. The values used (K_1, k_2, k_3, k_4) were within the range obtained with the original pTAC in this study (K_1 = 0.10–0.31, k_2 = 0.03–0.11, k_3 = 0.02–0.48, and k_4 = 0.01–0.10). In healthy human subjects the peak time was found to be within 20 min post-injection.[1,6,31] The peak count times of tTAC calculated from Eq. 4 were 7.5, 11.25, 22.5, 41.25, 60, 82.5, 101.25, 120, and 142.5 min. Counts were calculated in 3.65-min intervals from 0 min to 251.25 min. The tTAC used was continuous from 0 min to 251.25 min. The pTAC used was multiplied by 0.7 for 30–180 min post-injection in the original pTAC. We chose 0.7 as the multiplication factor, because the changes in the late period of pTAC showed that when f_m was 0.7, most BP_m values were estimated within 1.6 of BP_o. When the multiplication factor was less than 0.7, the difference was much larger.

Changes in peak count time of tTAC in clinical SPECT scans. Intermittent three dynamic SPECT was performed in this study instead of whole time scans. The possibility that peak brain activity might have been missed had to be considered. To adjust the clinical SPECT scans, counts of tTAC were picked up at 0–41.25 min, 90–112.5 min, and 180–202.5 min. Other conditions were the same as in previous simulations (Changes in peak count time of tTAC).

Additional arterial blood sampling

In data analysis with SIF, one artery blood sampling is

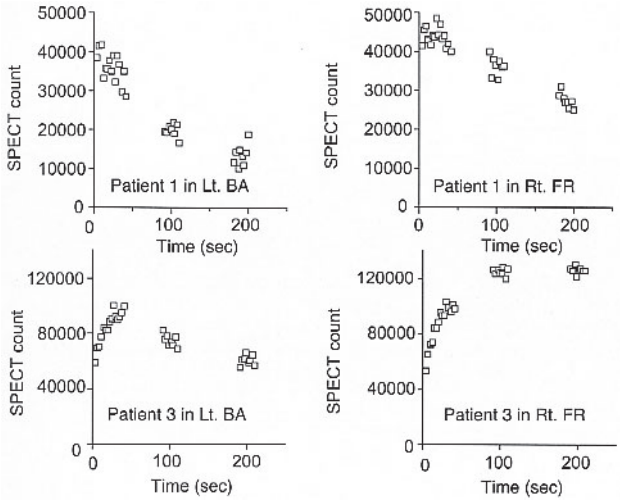

Fig. 3 SPECT counts of patients 1 and 3.
Lt. = left; Rt. = right; BA = basal ganglia; FR = frontal lobe.

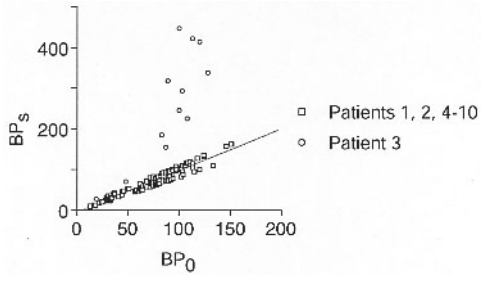

Fig. 4 Comparison of binding potential (BP) calculated with patient's original pTAC (BP_o) and BP calculated with SIF (BP_s). BP_o are shown along the *x*-axis. The values on the *y*-axis were obtained by 3-compartment-3-parameter analysis from SIF with calibration of the blood taken at 30 min post-injection of IMZ. The linear regression exists in patients 1, 2, 4–10 ($BP_s = 1.02BP_o - 3.9$).

used. To check whether another blood sampling increases the accuracy of calculation, we used additional arterial blood sampling at 180 min post-injection. Other conditions were the same as in the previous 3-compartment-3-parameter model analysis.

RESULTS

Nine of the 10 patients showed almost the same percentage decrease in plasma activity, but patient 3 showed a slower decrease (Fig. 2). The maximum count of tTAC was included in the first scan in the 9 patients, but the maximum count of tTAC in patient 3 was in the second or third SPECT scan in 9 ROIs (Fig. 3).

Comparison of SIF and original pTAC

Nine of the 10 patients showed a good correlation between BP calculated with patient's original pTAC (BP_o) ($r = 0.96$, $p < 0.0001$, $BP_s = 1.02BP_o - 3.9$) and BP calculated with SIF (BP_s), but the maximal BP_s to BP_o ratio in patient 3 was greater than six (Fig. 4).

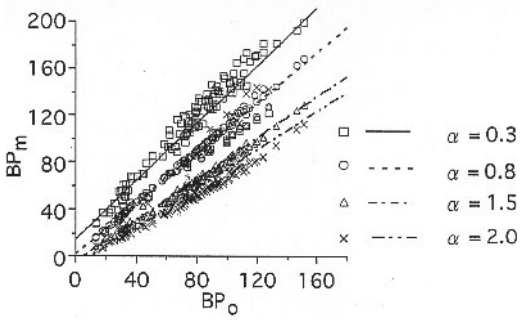

Fig. 5 Influence of changes in peak value of pTAC. BP in tissue was estimated by 3-compartment-3-parameter analysis. BP_os are shown along the *x*-axis. The values on the *y*-axis were obtained by using modified input functions of various peak values. The multiplication factors are 0.3, 0.8, 1.5, and 2.0 (Eq. 11–14). All data points were included in the linear regression: $BP_m = 1.23BP_o + 15.3$ when $\alpha = 0.3$; $BP_m = 1.08BP_o + 2.1$ when $\alpha = 0.5$; $BP_m = 0.88BP_o - 4.2$ when $\alpha = 1.5$; $BP_m = 0.82BP_o - 8.6$ when $\alpha = 2.0$.

Change in the level of pTAC in the early period

Except in patient 3, when α (Eq. 11–14) was less than one, BP_ss calculated from the modified pTAC (BP_m) were greater than BP_os. When α was greater than one, BP_ms were less than BP_os. The largest ratio of BP_m to BP_o was 2.12 when α was 0.3 ($BP_m = 1.23BP_o + 15.3$) (Fig. 5); the smallest ratio of BP_m to BP_o was 0.37 when α was 2.0 ($BP_m = 0.82BP_o - 8.6$).

These trends were not observed in patient 3. Whether BP_m was greater or less than BP_o depended on the region and α. The maximal difference between BP_m and BP_o was 23%.

Changes in count peak time of pTAC

BP_m values showed a good correlation with BP_o (Fig. 6) ($r = 0.99$, $p < 0.0001$) and BP_s (not shown). The maximal difference between BP_m and BP_o was 11% when the count peak time of pTAC was 0.3 min.

Changes in the late period of pTAC

BP_m with multiplication factor $f_m = 0.7$ and 1.1 correlated well with BP_o (Fig. 7) ($BP_m = 1.26BP_o - 3.5$, $r = 0.97$, $p < 0.0001$ when $f_m = 0.7$; $BP_m = 0.94BP_o - 0.5$, $r = 0.998$, $p < 0.0001$ when $f_m = 1.1$). The largest difference between BP_m and BP_o was 61% when f_m was 0.7 and 12% when f_m was 1.1. However, BP_m was very different when f_m was 0.4, and the largest ratio was 3.8. When the pTAC at 30–180 min had the same value at 30 min post-injection, BP_m was well correlated with BP_o, but its value was almost half that of BP_o ($BP_m = 0.51BP_o - 0.7$, $r = 0.97$, $p < 0.0001$).

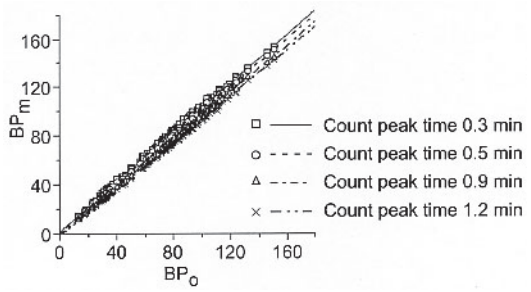

Fig. 6 Influence of changes in peak time of pTAC. BPs in tissue were estimated by 3-compartment-3-parameter analysis. BP_os are shown along the *x*-axis. The values on the *y*-axis were obtained by using modified input functions at various peak times of pTAC (0.3, 0.5, 0.9, and 1.2 min). A good correlation is observed. All data points were included in the linear regression: $BP_m = 1.01BP_o + 1.6$ when count peak time is 0.3 min; $BP_m = 1.00\,BP_o + 0.7$ when count peak time is 0.5 min; $BP_m = 0.94\,BP_o - 0.9$ when count peak time is 0.9 min; $BP_m = 0.96BP_o - 1.9$ when count peak time is 1.2 min.

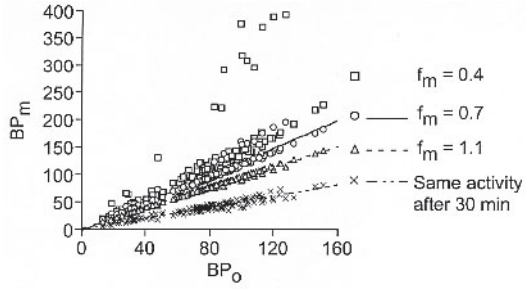

Fig. 7 Influence of changes in the later portion of pTAC. BPs of tracer in tissue were estimated by 3-compartment-3-parameter analysis. BP_os are shown along the *x*-axis. The values on the *y*-axis were obtained by using modified input function at various counts after 30 min post-injections of IMZ. The multiplication factor is 0.4, 0.7, or 1.1, and input functions with the same values after 30 min were used in the calculations. The linear regression is $BP_m = 1.26BP_o - 3.5$ when $f_m = 0.7$; $BP_m = 0.94BP_o - 0.5$ when $f_m = 1.1$; $BP_m = 0.51BP_o - 0.7$ when count of pTAC in the late period is the same value after 30 min.

Changes in peak count time of tTAC

As the peak count time of tTAC became later, the difference between BP_o and BP_m became larger (Fig. 8A). The largest difference between BP_m and BP_o was 57%, when the peak count time of tTAC was 140 min. When peak count time was 140 min, the difference between BP_m and BP_o was greater than 48% in all 10 patients.

Changes in peak count time of tTAC in clinical SPECT scans

As the peak count time of tTAC increased, the difference between BP_o and BP_m increased. When f_m was 0.7, the maximum difference between BP_m and BP_o was 1.92-fold at a peak count time of 140 min (Fig. 8B).

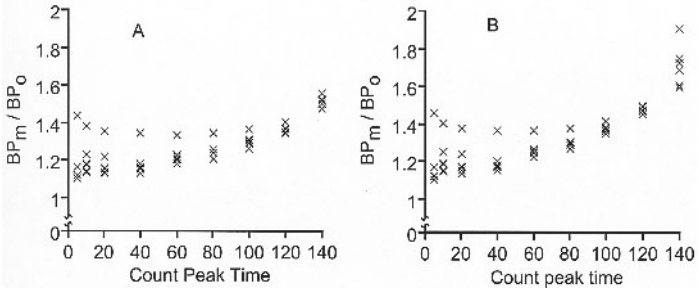

Fig. 8 (A) Influence of changes in peak count time. TAC in brain tissue (tTAC) used was continuous from 0 min to 251.25 min. (B) Influence of changes in peak count time in clinical SPECT scans (three intermittent dynamic SPECT scans). BPs of tracer in tissue were estimated by 3-compartment-3-parameter analysis. The values on the *x*-axis were the peak count time of tTAC. The values on the *y*-axis were the ratios BP_m to BP_o.

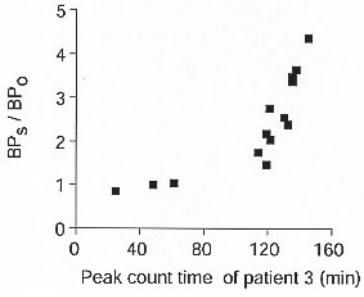

Fig. 9 The ratios BP_s to BP_o in patient 3. Peak count time was calculated from Eq. 3–6 (K_1, k_2, k_3, k_4, and the original input function).

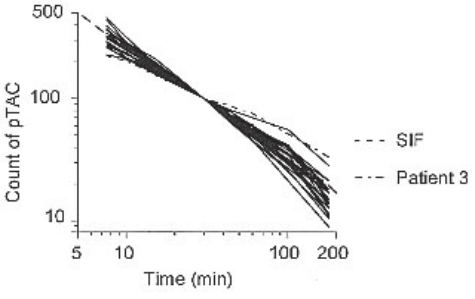

Fig. 10 The late period of pTAC of SIF and 26 patients. Counts shown in this figure are calibrated with the count at 30 min post-injection set equal to 100.

Additional arterial blood sampling

The mean BP_s/BP_o declined from 2.46 to 1.82 in patient 3 and from 0.96 to 1.02 in the other patients.

Table 1 K_1, k_2, k_3 and BP calculated from the original arterial curve of 10 patients

ROIs	K_1 (m*l* g^{-1} min^{-1})	k_2 (min^{-1})	k_3 (min^{-1})	BP
Frontal in patient 1, 2, 4–10	0.195 ± 0.017	0.065 ± 0.006	0.131 ± 0.049	84.7 ± 11.1
in patient 3	0.147 ± 0.022	0.015 ± 0.001	0.045 ± 0.001	72.0 ± 3.9
Temporal in patient 1, 2, 4–10	0.206 ± 0.031	0.069 ± 0.010	0.168 ± 0.037	85.6 ± 12.4
in patient 3	0.171 ± 0.001	0.025 ± 0.018	0.091 ± 0.077	92.3 ± 19.6
Parietal in patient 1, 2, 4–10	0.199 ± 0.031	0.066 ± 0.012	0.197 ± 0.085	78.7 ± 12.8
in patient 3	0.141 ± 0.018	0.012 ± 0.002	0.030 ± 0.004	56.1 ± 5.6
Occipital in patient 1, 2, 4–10	0.232 ± 0.031	0.077 ± 0.011	0.234 ± 0.069	82.5 ± 14.9
in patient 3	0.190 ± 0.004	0.012 ± 0.001	0.027 ± 0.001	65.9 ± 7.8
Cerebellum in patient 1, 2, 4–10	0.266 ± 0.064	0.089 ± 0.022	0.025 ± 0.008	90.3 ± 27.8
in patient 3	0.182 ± 0.014	0.106 ± 0.082	0.334 ± 0.288	87.0 ± 5.4
Thalamus in patient 1, 2, 4–10	0.178 ± 0.042	0.058 ± 0.012	0.035 ± 0.021	29.8 ± 7.7
in patient 3	0.145 ± 0.05	0.130 ± 0.140	0.153 ± 0.178	25.2 ± 14.8
Basal ganglia in patient 1, 2, 4–10	0.200 ± 0.037	0.067 ± 0.012	0.047 ± 0.063	41.5 ± 16.6
in patient 3	0.188 ± 0.115	0.282 ± 0.369	0.268 ± 0.320	36.6 ± 3.7

Values represent ± Mean SD.

BP means "binding potential," and k_4 was estimated to be 0.026 min^{-1}.

DISCUSSION

The results of our study showed that SIF can serve as an alternative true arterial curve in the 3-compartment-3-parameter model when (a) the rate of count decrease after 30 min post-injection is close to that of SIF (within 40%), or (b) the time of peak brain radioactivity is less than 100 min.

Under clinical SPECT scan conditions, if the rate of count decrease in pTAC is less than that of SIF after 30 min post-injection, BP_s becomes greater than BP_o. When the multiplication factor f_m (Eq. 16) was greater than 0.7, BP_m was well correlated with BP_o in our preliminary calculations. In contrast, when the multiplication factor was less than 0.6, in patient 3 BP_m was three times as high as BP_o (Fig. 7). In this case, the peak count times were longer than 105 min.

When the peak count time was longer than 100 min, the difference between BP_m and BP_o was greater than 30%. Identifying the exact peak time is important for kinetic analysis. In patient 3, the ROIs that showed very large differences (greater than 200%) between BP_m and BP_o were the frontal, occipital, and temporal lobes, where the peak count time seemed to be between 100 and 190 min. The basal ganglia and thalamus, where peak count time seemed to lie between 20 and 50 min, did not show any great differences (less than 150%).

In clinical SPECT scans, in which measurements are made in two or three separate scans, the difference between BP_o and BP_m becomes greater than when continuous SPECT scans are taken. It is impossible to determine the peak count time exactly. Even when the peak count time is 80 min, if the SPECT scans are taken at 0–42 min and 180–201 min, the maximum difference of BP_m against BP_o is 37%. If SPECT scans are taken at 0–42 min, 90–111 min, and 180–201 min, the difference is 27%. If the peak count time is within the first SPECT scan time, the difference between BP_o and BP_m is less than 20%, and is almost the same as for continuous SPECT scans.

The ratio of BP_s to BP_o in patient 3 increased dramatically when the peak count time exceeded 100 min (Fig. 9). When the arterial curve decreases at almost the same rate as SIF, the peak count time does not exceed 100 min in clinical measurements. Even when simulated in Eq. 4, the peak count time cannot exceed 130 min within the limitations of normal BP. If the peak count time exceeds 120 min in clinical measurements, the rate of decrease in the original arterial curve after 30 min post-injection can be concluded to be smaller than SIF. Kinetic analyses with SIF should be applied on the condition that the peak count time is within 100 min. When the arterial curve decreases faster than SIF, the peak count time should become shorter. In this situation, a correct BP would be obtained with SIF in our preliminary simulation. Thus, only situations in which there is a slow decrease rate after calibration time adversely affect simulations in kinetic analyses. Our IMZ SPECT scan data in 34 patients and pTAC in 26 patients showed a slow count decrease rate after calibration time in two patients (including patient 3) (Fig. 10). This exception occurred in 6% of our patients.

The standardized input function approach entails several potential sources of errors.

1) Extravasation of some or all of the tracer. When a subject receives an intravenous bolus injection, some of the tracer may remain under the subcutaneous tissue or in muscle.
2) Altered tracer arrival in the brain. If a subject has heart disease (VSD, ASD, cardiac insufficiency) or an artery-to-vein shunt, the subject's arterial curve will differ from the SIF.

3) Altered plasma protein binding. If a patient has renal or hepatic failure, or is malnourished, plasma protein binding changes.
4) Abnormal tracer metabolism.

Hepatic failure or ingestion of some antipsychotic drugs may alter tracer metabolism in the blood or brain tissue. Our data for 26 artery curves showed that peak artery curve time ranged from 30 to 40 sec post-injection. The ratio of the peak artery values to the values on the calibration time (at 30 min in our cases) ranged from 53.5 to 230.4, and the ratio of artery values at 180 min to the values on the calibration time ranged from 0.017 to 0.32. In clinical studies that include patients with severe heart disease, renal failure, or hepatic failure, these ranges may become wider. In our study, no patients had severe heart disease, renal failure, or hepatic failure; however, we believe our simulation was effective with these limitations. The standard input curve used in our data was plotted from data obtained from relatively young subjects (24–61 years old). Because tracer clearance changes with age,[32] a standard input function created from middle aged and aged subjects may improve the reliability of the single blood sample method.

The reasons for the great differences between BP_o and BP_s in some ROIs in patient 3 are unknown. The calculated K_1, k_2, k_3, k_4, and BP_o values in patient 3 were not different from those in other patients (Table 1). The differences were mainly due to the longer peak count times than in the other patients and volunteers and to the slow decrease rate after calibration time. The patient showed no evidence of heart failure, renal failure, lung abnormalities, or liver failure, and he was not a smoker. We were unable to obtain this patient's delayed peak count time either during SPECT acquisition or in arterial blood sampling before the clinical SPECT scan. His BP_os were within the normal range when calculated from his own counts and his own arterial curve. If a leak had occurred at the site of injection of IMZ, the peak count times would have occurred later in all of the ROIs, but the peak count times in the left basal ganglia, right thalamus, and bilateral occipital lobes occurred within 50 min. We could not exclude the possibility of extravasation in patient 3, but no extravasation of the tracer injection was seen on the actual IMZ SPECT scan, and the patient did not complain of pain at the site of the injection. Acquisition of some of the brain data (right frontal lobe, bilateral occipital lobe, and left parietal lobe) in patient 3 was terminated around the peak, and measurements of binding potential based on these data may be unreliable. However, Eq. 3 and Eq. 4 can be solved without the limitation of the shape of the ligand concentration curve in arterial plasma, and the calculated K_1, k_2, k_3 and BP values were not outliers (Table 1).

Since the differences between BP_o and BP_m were very large in patient 3, it was clear that the results of the calculations were doubtful. However, if the differences were smaller in other cases without sequential blood samplings, these wrong calculations can be overlooked. When automatically calculating BP maps, it is impossible to confirm whether the values are reliable, because it is difficult to check peak times in clinical measurements. If the difference is small, or the peak count time is less than 100 min, the difference can be overlooked. When the individual patient's arterial curve has the same shape as the curve of the reference population, the method with SIF is successful, but it fails when the shape differs, as in patient 3. This occurs relatively frequently in clinical settings, particularly with uncooperative or demented neurological patients.

There are some alternatives to the strategy which could yield IMZ BP measurements without the need for arterial blood sampling. Laruelle et al.[33] described a constant infusion approach involving IMZ infusion until brain-to-blood equilibrium is established. In their procedure, the static pattern of IMZ distribution is directly proportional to BP. The subject is injected with high affinity IMZ, and a receptor-saturating dose of flumazenil at the end of a measurement to measure nondisplaceable activity. This method requires two ligands. Logan[34] and Lammertsma [35] independently described a reference region approach involving only dynamic brain imaging. Logan used [^{11}C]raclopride and [^{11}C]d-threo-methylphenidate, and Lammertsma used [^{11}C]raclopride. These methods use data from a nonreceptor region. A map of relative tissue volumes of distribution can be made by transforming the scan data. This is proportional to BP. There are no proper regions with sufficiently low benzodiazepine receptors. Even though the pons, which is sometimes used as a receptor-poor region, displays a considerable amount of specific receptors,[21] one could assume that a fixed fraction of the pons was free or nonspecific binding.

There were some limitations to our study: (1) parameters were obtained by sequential quadratic programming, where the extent of the parameters is constrained; (2) the compartment analysis used in this study was based on 3-compartment-3-parameters; (3) when checking the influence of the peak count time, some kinetic parameters were fixed ($K_1/k_2 = 3$); (4) arterial curves were obtained from plasma after octanol extraction, whereas SIF was obtained from plasma after chloroform extraction; and (5) the calibration of the arterial curves was based on count values at 30 min post-injection. We do not think that (1) is a major problem. A nonlinearly constrained problem can often be solved in less iteration by using semisequential quadratic programming than an unconstrained problem. When making real estimates, parameters in tracer kinetics entail certain constraints. As for (2) and (3), we calculated the parameters by 3-compartment-2-parameter analysis and 3-compartment-4-parameter analysis in several ROIs of patient 3, and we also calculated BP by 3-compartment-3-parameters where k_4 was assumed to be 0.024. The

results obtained were almost the same as those obtained in this study. As for (4), all patients but patient 3 showed a good correlation between BP_o and BP_s. Therefore, arterial curves obtained after octanol extraction can be used instead of curves obtained by chloroform extraction. As for (5), we did not check any calibration times other than 30 min, and thus, the best calibration time may not be 30 min post-injection.[36]

Our simulation of changes in the late period of pTAC showed the rate of count decrease was important for precise calculation of BP. The late period of pTAC (Fig. 10) can be estimated from two points sampling (Fig. 10). To decrease the difference between BP_o and BP_s, we used one blood sampling after 30 min post-injection (for example after the second or third SPECT scan). An arterial curve at 0–30 min is obtained by calibration of SIF by arterial blood sampling at 30-min, and from 30 min to the endpoint the decay ratio is adjusted by using 30-min samples and samples at another time.

Using additional arterial blood data at 180 min post-injection reduced the mean BP_s/BP_o. This means that the difference between BP_o and BP_m was decreased greatly by two point blood sampling. This two point sampling method does not decrease the influence of the peak plasma value (Fig. 5), but we believe that it is effective in decreasing calculation errors. In an iodine-123 IMP cerebral blood flow study, venous sampling from the dorsal hand was proposed instead of arterial blood sampling.[37] This venous sampling method might be used instead of arterial sampling to obtain a patient's individual arterial curve in an IMZ study.

CONCLUSIONS

In conclusion, the standard input function can be used instead of the patient's own arterial curve to calculate BP on condition that: (a) the rate of count decrease after 30 min post-injection is close to that of SIF (within 40%), or (b) the time of peak brain radioactivity is less than 100 min. Height in the late scan period can produce significant errors in estimated BPs. A single blood sampling is insufficient to adjust the standardized blood input curve for IMZ BP calculation. We recommend one or more additional blood samplings after the calibration time or a reference region approach.

In this paper we used IMZ as the receptor ligand. In kinetic models with ligands having longer decay times of more than several hours, like IMZ, the count of the arterial curve in the late period is important when calculating by the standard input function instead of the patient's own arterial curve.

Two or more sampling methods may be useful to increase accuracy in a kinetic model with standard input function in SPECT studies with ligands having longer decay times of more than several hours.

ACKNOWLEDGMENT

The authors thank Nihon Medi-Physics Co., Ltd. for providing IMZ.

REFERENCES

1. Holl K, Deisenhammer E, Dauth J, Carmann H, Schubiger PA. Imaging benzodiazepine receptors in the human brain by single photon emission computed tomography (SPECT). *Int J Rad Appl Instrum B* 1989; 16: 759–763.
2. Beer HF, Blauenstein PA, Hasler PH, Delaloye B, Riccabona G, Bangerl I, et al. *In vitro* and *in vivo* evaluation of iodine-123-Ro 16-0154: a new imaging agent for SPECT investigations of benzodiazepine receptors. *J Nucl Med* 1990; 31: 1007–1014.
3. Johnson EW, Woods SW, Zoghbi S, McBride BJ, Baldwin RM, Innis RB. Receptor binding characterization of the benzodiazepine radioligand ^{125}I-Ro16-0154: potential probe for SPECT brain imaging. *Life Sci* 1990; 47: 1535–1546.
4. Innis RB, al Tikriti MS, Zoghbi SS, Baldwin RM, Sybirska EH, Laruelle MA, et al. SPECT imaging of the benzodiazepine receptor: feasibility of *in vivo* potency measurements from stepwise displacement curves [see comments]. *J Nucl Med* 1991; 32: 1754–1761.
5. Innis R, Zoghbi S, Johnson E, Woods S, al Tikriti M, Baldwin R, et al. SPECT imaging of the benzodiazepine receptor in non-human primate brain with [^{123}I]Ro 16-0154. *Eur J Pharmacol* 1991; 193: 249–252.
6. Woods SW, Seibyl JP, Goddard AW, Dey HM, Zoghbi SS, Germine M, et al. Dynamic SPECT imaging after injection of the benzodiazepine receptor ligand [^{123}I]iomazenil in healthy human subjects. *Psychiatry Res* 1992; 45: 67–77.
7. Savic I, Persson A, Roland P, Pauli S, Sedvall G, Widen L. *In-vivo* demonstration of reduced benzodiazepine receptor binding in human epileptic foci. *Lancet* 1988; 2: 863–866.
8. Johnson EW, de Lanerolle NC, Kim JH, Sundaresan S, Spencer DD, Mattson RH, et al. "Central" and "peripheral" benzodiazepine receptors: opposite changes in human epileptogenic tissue. *Neurology* 1992; 42: 811–815.
9. Kiuchi Y, Kobayashi T, Takeuchi J, Shimizu H, Ogata H, Toru M. Benzodiazepine receptors increase in post-mortem brain of chronic schizophrenics. *Eur Arch Psychiatry Neurol Sci* 1989; 239: 71–78.
10. Benes FM, Vincent SL, Alsterberg G, Bird ED, SanGiovanni JP. Increased $GABA_A$ receptor binding in superficial layers of cingulate cortex in schizophrenics. *J Neurosci* 1992; 12: 924–929.
11. Schlegel S, Steinert H, Bockisch A, Hahn K, Schloesser R, Benkert O. Decreased benzodiazepine receptor binding in panic disorder measured by IOMAZENIL-SPECT. A preliminary report. *Eur Arch Psychiatry Clin Neurosci* 1994; 244: 49–51.
12. Schroder J, Silvestri S, Bubeck B, Karr M, Demisch S, Scherrer S, et al. D2 dopamine receptor up-regulation, treatment response, neurological soft signs, and extrapyramidal side effects in schizophrenia: a follow-up study with ^{123}I-iodobenzamide single photon emission computed tomography in the drug-naive state and after neuroleptic treatment. *Biol Psychiatry* 1998; 43: 660–665.
13. Onodera H, Sato G, Kogure K. GABA and benzodiazepine

receptors in the gerbil brain after transient ischemia: demonstration by quantitative receptor autoradiography. *J Cereb Blood Flow Metab* 1987; 7: 82–88.
14. Penney JB Jr, Young AB. Quantitative autoradiography of neurotransmitter receptors in Huntington disease. *Neurology* 1982; 32: 1391–1395.
15. Walker FO, Young AB, Penney JB, Dovorini Zis K, Shoulson I. Benzodiazepine and GABA receptors in early Huntington's disease. *Neurology* 1984; 34: 1237–1240.
16. Whitehouse PJ, Trifiletti RR, Jones BE, Folstein S, Price DL, Snyder SH, et al. Neurotransmitter receptor alterations in Huntington's disease: autoradiographic and homogenate studies with special reference to benzodiazepine receptor complexes. *Ann Neurol* 1985; 18: 202–210.
17. Mintun MA, Raichle ME, Kilbourn MR, Wooten GF, Welch MJ. A quantitative model for the *in vivo* assessment of drug binding sites with positron emission tomography. *Ann Neurol* 1984; 15: 217–227.
18. Perlmutter JS, Larson KB, Raichle ME, Markham J, Mintun MA, Kilbourn MR, et al. Strategies for *in vivo* measurement of receptor binding using positron emission tomography. *J Cereb Blood Flow Metab* 1986; 6: 154–169.
19. Koeppe RA, Holthoff VA, Frey KA, Kilbourn MR, Kuhl DE. Compartmental analysis of [^{11}C]flumazenil kinetics for the estimation of ligand transport rate and receptor distribution using positron emission tomography. *J Cereb Blood Flow Metab* 1991; 11: 735–744.
20. Holthoff VA, Koeppe RA, Frey KA, Paradise AH, Kuhl DE. Differentiation of radioligand delivery and binding in the brain: validation of a two-compartment model for [^{11}C]flumazenil. *J Cereb Blood Flow Metab* 1991; 11: 745–752.
21. Abi Dargham A, Laruelle M, Seibyl J, Rattner Z, Baldwin RM, Zoghbi SS, et al. SPECT measurement of benzodiazepine receptors in human brain with iodine-123-iomazenil: kinetic and equilibrium paradigms. *J Nucl Med* 1994; 35: 228–238.
22. Abi Dargham A, Gandelman M, Zoghbi SS, Laruelle M, Baldwin RM, Randall P, et al. Reproducibility of SPECT measurement of benzodiazepine receptors in human brain with iodine-123-iomazenil. *J Nucl Med* 1995; 36: 167–175.
23. Onishi Y, Yonekura Y, Mukai T, Nishizawa S, Tanaka F, Okazawa H, et al. Simple quantification of benzodiazepine receptor binding and ligand transport using iodine-123-iomazenil and two SPECT scans. *J Nucl Med* 1995; 36: 1201–1210.
24. Buck A, Westera G, vonSchulthess GK, Burger C. Modeling alternatives for cerebral carbon-11-iomazenil kinetics. *J Nucl Med* 1996; 37: 699–705.
25. Yonekura Y, Nishizawa S, Tanaka F, Ishizu K, Okazawa H, Fujita T, et al. Phase 1 clinical study of ^{123}I-iomazenil: a new probe to evaluate central-type benzodiazepine receptor with SPECT. *KAKU IGAKU (Jpn J Nucl Med)* 1995; 32: 87–97.
26. McKhann G, Drachman D, Folstein M, Katzman R, Price D, Stadlan EM. Clinical diagnosis of Alzheimer's disease: report of the NINCDS-ADRDA Work Group under the auspices of Department of Health and Human Services Task Force on Alzheimer's Disease. *Neurology* 1984; 34: 939–944.
27. Zoghbi SS, Baldwin RM, Seibyl JP, al-Tikriti MS, Zea-Ponce Y, Laruelle M, et al. Pharmacokinetics of the SPECT benzodiazepine receptor radioligand [^{123}I]iomazenil in human and non-human primates. *Int J Rad Appl Instrum B* 1992; 19: 881–888.
28. Phelps ME, Huang SC, Hoffman EJ, Kuhl DE. Validation of tomographic measurement of cerebral blood volume with C-11-labeled carboxyhemoglobin. *J Nucl Med* 1979; 20: 328–334.
29. Gill PE, Murray W, Sanders MA, Wright MH. Procedures for Optimization Problems with a Mixture of Bounds and General Linear Constraints. *ACM Trans Math Software* 1984; 10: 282–298.
30. Schittowski K. NLQPL: A FORTRAN-subroutine Solving Constrained Nonlinear Programming Problems. *Operations Research* 1985; 5: 485–500.
31. Dey HM, Seibyl JP, Stubbs JB, Zoghbi SS, Baldwin RM, Smith EO, et al. Human biodistribution and dosimetry of the SPECT benzodiazepine receptor radioligand iodine-123-iomazenil. *J Nucl Med* 1994; 35: 399–404.
32. Bruno B, Ilaria B, Pliergiuseppe O, Tolmino C. How gender and age affect Iodine-131-OIH and Technetium-99m-MAG3 clearance. *J Nucl Med Technol* 2000; 28: 156–158.
33. Laruelle M, Abi Dargham A, al Tikriti MS, Baldwin RM, Zea Ponce Y, Zoghbi SS, et al. SPECT quantification of [^{123}I]iomazenil binding to benzodiazepine receptors in nonhuman primates: II. Equilibrium analysis of constant infusion experiments and correlation with *in vitro* parameters. *J Cereb Blood Flow Metab* 1994; 14: 453–465.
34. Logan J, Fowler JS, Volkow ND, Wang GJ, Ding YS, Alexoff DL. Distribution volume ratios without blood sampling from graphical analysis of PET data. *J Cereb Blood Flow Metab* 1996; 16: 834–840.
35. Lammertsma AA, Hume SP. Simplified reference tissue model for PET receptor studies. *Neuroimage* 1996; 4: 153–158.
36. Ito H, Goto R, Koyama M, Kawashima R, Ono S, Sato K, et al. A simple method for the quantification of benzodiazepine receptors using iodine-123 iomazenil and single-photon emission tomography. *Eur J Nucl Med* 1996; 23: 782–791.
37. Ito H, Koyama M, Goto R, Kawashima R, Ono S, Atsumi H, et al. Cerebral blood flow measurement with iodine-123-IMP SPECT, calibrated standard input function and venous blood sampling [see comments]. *J Nucl Med* 1995; 36: 2339–2342.